CORROSION OF STRUCTURAL MATERIALS IN DYNAMIC LITHIUM

F. CASTEELS, H. TAS, J. DEKEYSER, M. SOENEN, F. LIEVENS

Studiecentrum voor Kernenergie, S.C.K./C.E.N.,
Boeretang 200, B-2400 Mol, Belgium

Abstract

Corrosion tests have been carried out on AISI 304, AISI 304L, AISI 316, AISI 316L and carbon steel in the hot (400°C) and cold (355°C) sections of the Li-1 loop with a content of 40 l. The loop is made from AISI 316 steel. The maximum duration of lithium experiments under identical conditions of temperature and velocity reached 7275 h.

The lithium velocity varied between 0.12 $m.s^{-1}$ and 0.27 $m.s^{-1}$ during the low-velocity experiments. In the high-velocity experiments, these values are in the range between 1.68 $m.s^{-1}$ and 2.375 $m.s^{-1}$. The lithium has been purified by cold and hot trapping. Cold trapping is not effective for nitrogen and hot trapping starts to be effective in this respect using Ti sponge at temperatures of 600°C. The corrosion rate is found to be a function of cold trap temperature, lithium velocity, exposure temperature and to a minor extent of alloy composition and the pre-corrosion heat treatment. Increasing the lithium velocity from 0.14 $m.s^{-1}$ to 2.375 $m.s^{-1}$ enhances the corrosion rate of AISI 316 steel from 1.10^{-5} $m.a^{-1}$ to 7.10^{-5} $m.a^{-1}$. Hot trapping at 600°C reduces the corrosion rate from 7.10^{-5} $m.a^{-1}$ to 3.10^{-5} $m.a^{-1}$.

A porous ferritic subsurface layer is formed on the specimens corroded in the hot sections of the loop. The thickness of this ferritic layer at 400°C reaches about 10^{-5}m and is practically independent of exposure time, alloy composition of austenitic grades, pre-corrosion heat treatment and lithium velocity. The formation of the corrosion layer is due to the selective leaching of alloy constituents such as chromium, nickel, molybdenum, manganese and silicon in lithium and the pick-up of calcium, lithium, carbon and nitrogen from the lithium. The ferrite layer formed at 400°C on type AISI 316 steel is pure iron alloyed with 1 wt.% carbon, nitrogen, some calcium and a lithium compound in the pores.

Crystalline iron-rich deposits are present in the cold-temperature test section. The deposition layer has a porous structure and a very irregular thickness varying between 2.10^{-6} m and 10^{-5} m after 7275 h exposure at 355°C. The deposit is mainly composed of pure iron alloyed with 0.5 wt.% carbon.

1. Introduction

Liquid lithium is considered to be a strong candidate for both the coolant and breeding blanket material for the controlled thermonuclear reactor. Only limited data exist on the behaviour of structural materials in dynamic lithium and most of them are obtained in chemically undefined lithium in thermal convection loops [1]. Impurities of lithium which have to be taken into account in the corrosion process are oxygen, carbon, nitrogen and hydrogen [1]. For long-term application, austenitic stainless steels appear up to now to be limited to about 500°C. Corrosion can probably be decreased to lower values and the aim of present study is to give a contribution to the reduction of the corrosion rate to predictable and tolerable amounts. A complete understanding of the kinetics of all reactions contributing to the corrosion mechanism is of great importance. This includes the knowledge of interactions between nitrogen, carbon, oxygen and hydrogen present in the lithium and in the alloy, the rate of second phase formation and the solution rate of alloy constituents in lithium with a well-defined quality.

2. Experimental techniques

The study of corrosion rate and mechanism, mass transfer and deposition phenomena is based on long-term high and low velocity experiments in a non-isothermal loop with two parallel test sections in the hot part of the loop and two parallel test sections in the cold part of the loop.

Besides these four test sections the main circuit includes : an electromagnetic pump, a Li-Li recuperator, an electrical heater of 50 kW, an expansion tank, a lithium-air cooler, an electromagnetic flow-meter, and another Li-Li recuperator. The purification system and the plugging system consist of a cold and hot trap and a plugging valve with a perforated seat. The hot trap consists of Ti-sponge or Fe-Ti alloys exposed at 400°C or 600°C to dynamic lithium ; the hot trap has to be used since the purification of nitrogen with cold trapping is quite ineffective due to the high solubility of nitrogen even at the melting point of lithium [2].

The analysis of the corrosion tested materials is given in Table I. The low-velocity high-temperature test section and the low-velocity low-temperature test section contain 10 samples. In the high-velocity high-temperature test section the samples are inserted two by two at 3 mm distance. The total length of this test section is 0.22 m. The test samples were fabricated from rolled material and have following dimensions 65 ± 0.1 x 12 ± 0.1 x 2 ± 0.01 mm. After degreasing, ultrasonic cleaning in ethyl alcohol, the samples have been weighed.

The test temperature was 400°C in the hot section of the loop and the test section in the low temperature of the loop was operated at 355°C. The lithium velocity varied between 0.12 $m.s^{-1}$ and 0.27 $m.s^{-1}$ during the low-velocity experiments and between 2.375 $m.s^{-1}$ and 1.68 $m.s^{-1}$ during the high velocity experiments.

The velocity in the cold temperature test section varied between 0.03 and 0.133 $m.s^{-1}$.

After removal from the lithium loop, the specimens were cleaned by washing in distilled water. The maximum duration of the lithium experiments lasted 7275 h and 5659 h respectively in the low and high velocity experiments.

Periodic analyses of the nitrogen, carbon, oxygen and metallic impurities in the lithium have been carried out. Nitrogen has been determined using the micro-Kjeldahl method. Carbon and carbon carriers have been determined by the method established for sodium [3]. Metallic

impurities have been determined using X-ray fluorescence techniques.

3. Experimental results

3.1. Gettering of the lithium

Since nitrogen, carbon, oxygen and to a lesser extent hydrogen influence the compatibility of stainless steels with liquid lithium, purification techniques have to be used to obtain acceptable purity levels in lithium. The solubility of interstitial elements such as nitrogen, carbon, oxygen and nitrogen is high even at the melting point of lithium [2]. The effectiveness of cold trapping has been evaluated by chemical analysis of the lithium. It has been found that the nitrogen content of the Li, which considerably affects the solubilities of important components (Ni, Cr, Fe) of stainless steel in Li, could not be reduced to a sufficiently low level. Carbon originating either from the steel or from the lithium is responsible for intergranular corrosion in austenitic stainless steels. Rather high carbon contents remain in the lithium after cold trapping. Oxygen is responsible for the initial solution rate of steels. Reasonably low oxygen levels can be maintained in lithium by cold trapping.

Since nitrogen cannot be eliminated by cold trapping trials have been undertaken to purify lithium from nitrogen by a chemical gettering technique.

With titanium, nitrogen gettering is thermodynamically possible at 400°C [4]. As indicated in Table II, it turned out that at this temperature the reaction kinetics are too low. The nitrogen content in the lithium remains high.

Gettering at 600°C for 1209 h using 200 g Ti sponge resulted in an average of 55,000 ppm nitrogen at the outer surface and 38,000 ppm in the inner body of the getter. The gettering efficiency at 600°C is about a factor 100 higher than at 400°C. The Ti sponge not only getters nitrogen but also to a lesser amount and in decreasing order of importance, oxygen, hydrogen and carbon. Microprobe analysis carried out on the bulk material and the nitride phase of the Ti-sponge revealed between 0.03 and 3.49 at.% nitrogen in the bulk material of the Ti-sponge. The nitride phase contains between 26.67 at.% and 39.75 at.% nitrogen.

Cast Fe-Ti alloys with different compositions (Fe 1,5, 7 and 25 wt.% Ti) have been tested to examine the effectiveness of these alloys. Nitrogen pick-up for the Fe-1,5,7% Ti alloys amounted to about 10 times the blank and for the Fe-25% Ti to about 20 times. The Fe-Ti alloys picked up a much larger amount of oxygen. The low values obtained for the pick-up of nitrogen is probably due to the fact that Fe-Ti alloys are not available in the form of a sponge and that an impervious oxinitride layer forms on their surface. An overview of the results of periodic analyses of nitrogen and carbon in the lithium is given in Table II. The duration time of the different test periods and the time with a cold trap temperature above 190°C are given in Table III. A high cold trap temperature being a measure for higher corrosiveness of the lithium.

3.2. Corrosion phenomena

3.2.1. Weight measurements

Weight losses have been observed for all austenitic stainless steels and for the carbon steel tested in the hot test section. The weight changes in the high temperature test section as a function of material, pre-corrosion heat treatment, exposure time and velocity are represented in Tables IV.A and IV.B. The corrosion rate for the high velocity experiments is largely dependent on the nitrogen gettering capacity of the Ti-sponge and

the Fe-Ti alloys and the resulting nitrogen content of the lithium (Table IV.B). Exposure of pre-corroded steels in less pure lithium results in higher corrosion rates. Whereas carbon steel corrodes at a much higher rate than AISI 316, AISI 316L, AISI 304 and AISI 304L, AISI 304L possesses the highest corrosion resistance of the tested austenitic stainless steel family. The tests during period 4 (Table IV.A) have been carried out in the impurest lithium of all test periods (longest test period with high cold trap temperature). All steels corrode in this experimental conditions at 400°C at a corrosion rate of about 20.10^{-6} m.a^{-1}.
At a constant cold trap temperature of 190°C, the corrosion rate is decreased by a factor two. Increasing the lithium velocity from 0.15 m.s^{-1} to 2.375 m.s^{-1} enhances the corrosion rate by a factor of seven (from 10 m.10^{-6}.year^{-1} to 70 m.10^{-6}.year^{-1}).More effective gettering techniques can reduce the corrosion rate by a factor of 2.5 (Table IV.B test periods 9 and 10).

3.2.2. Metallographic changes

3.2.2.1. Structure of bulk material

Long-term exposure of AISI 304, AISI 304L, AISI 316, AISI 316L and carbon steel at temperatures of 1040°C, 700°C and 400°C can result in the precipitation of intermetallic and interstitial compounds. The amount and distribution of interstitial and to a lesser amount of intermetallic compounds can influence the extent of corrosion induced microstructural changes (e.g. intergranular attack).
The thermal effect of the long term corrosion treatment at 400°C has no significant influence on the structure established by the high-temperature pre-corrosion treatments.
The 700°C heat treatment results in development of carbide-decorated grain boundaries. The amount of carbides present on the grain boundaries is in correspondence with the interstitial content of the alloy. The grain boundaries are practically free from precipitates in AISI 304L. The nitrogen-rich AISI 316L steel revealed a practically continuous network of interstitial compounds on the grain boundaries.
The carbon steel revealed after the test a one-phase structure. Li-bearing compounds are found to be present in the bulk of the lithium corroded samples.

3.2.2.2. Corrosion-induced microstructural changes

Preferential depletion of substitutional elements especially at the grain boundaries and loss or pick-up of interstitial elements has an influence on the microstructure of the alloy in the surface and subsurface layers of the lithium exposed surface. Selective leaching of alloying elements such as chromium, nickel, molybdenum, manganese and silicon and the pick-up of interstitial elements such as nitrogen and carbon causes nucleation and growth of a porous continuous surface ferrite layer followed by grain boundary ferrite or grain boundary attack deeper in the material.
It has been found that a porous ferritic subsurface layer is formed on the specimens corroded at 400°C in the hot section of the loop. As illustrated in Figure 1 the thickness of the ferritic layer is about 10^{-5} m and is practically independent of exposure time, lithium velocity and alloy composition of austenitic grades.
At 600°C the ferritic subsurface layer reaches a thickness of 15.10^{-5}m after 1200 h of exposure. The dimensions of the pores present in the ferritic zone are smaller at lower exposure temperatures and diminish with increasing distance from the lithium-steel interface. The dimensions of the pores are dependent from the nature of the austenitic alloy ; a great-

er number of smaller pores are present in type AISI 316 steel than in AISI 304, where a small number of larger pores is present.
At isolated places the porous ferritic layer is separated from the unaffected matrix by a more dense ferritic phase. The ferritic layer is porous up to the surface or is separated from the surface by a 2.10^{-6} to 4.10^{-6} m thick ferrite layer practically free of voids.
Inert gas welds showed considerable attack although the ferritic phase present in the weld is more resistant to the lithium than the austenitic phase.
A continuous subsurface layer is not present on lithium corroded carbon steel. The cementite phase present in the as-received condition completely dissolves in the lithium.

3.2.2.3. Chemical changes

Concentration-penetration profiles have been determined by microprobe analysis, the RSV method as described by H.Schneider [5] and wet chemical analyses of corroded thin foil specimens. Surface concentrations of substitutional and interstitial elements have been derived from analyses obtained by the RSV method. The composition of individual phases has been derived from microprobe analysis. The formation of the corrosion layers is due to the selective leaching of alloying elements such as chromium, nickel, molybdenum, manganese and silicon and the pick-up of calcium, lithium, carbon and nitrogen in and from the lithium. The ferrite layer formed at 400°C on type AISI 316 is practically pure iron alloyed with 1 wt.% carbon, 1 wt.% nitrogen and some calcium. Lithium is found to be present in the subsurface layer. The composition of the different layers formed on type AISI 316 and AISI 304 steel is given in Table VI. The selective leaching of chromium and nickel is more pronounced for type AISI 316 steel than for AISI 304 steel. At isolated places the continuous ferritic layer is separated from the matrix by a phase with the following composition Fe = 75.77 wt.% ; Cr = 20.52 wt.% ; Mo = 2.40 wt.% ; Si = 0.08 wt.% ; Mn = 0.29 wt.% ; Ni = 0.93 wt.%.

3.2.2.4. Structural and scanning electron microscope analyses

The surface of the corroded samples has been examined by X-ray analysis and by a scanning electron microscope equipped with an EDAX-system. X-ray analyses revealed the presence of α-Fe at the surface of all corroded specimens. Holes are formed from the inner side of the samples in the direction of the surface. The surface layer is rich in iron and contains small amounts of chromium. The chromium content is higher in type AISI 304 steel than in AISI 316 steel corroded in identical conditions. The chromium content of the surface decreases with increasing exposure time. Two other kinds of particles are also present : particles rich in Ca and alloyed with Mg, Si, S and Cl and others which are rich in Fe and alloyed with Cr, Si and Ca.

3.3. Deposition phenomena

3.3.1. Weight measurements

The results of the deposition rate as a function of exposure time, alloy composition and pre-corrosion heat treatment of the steel samples in the low and high velocity experiments are represented in Tables V.A and V.B. The nucleation and growth of the first deposits has an effect on the deposition rate at the start of the experiment. The corrosion rates measured in the hot section have a dominating effect on the deposition rate measured in the cold section of the leg. The measured deposition rates give only a rough idea of the real deposition kinetics since the deposits have a non adherent character. Effective gettering of

the lithium reduces considerably the deposition rate (compare deposition rates during test periods 9 and 10).

3.3.2. Deposition induced microstructural changes

Deposition reactions, which occur in cooler regions may have substantial effects on overall heat transfer coefficients. A study of details of morphology, composition, porosity and interaction with the substrate will be dealt with in further paragraphs. The exact knowledge of the composition and structure of the species deposited in cold sections of a CTR loop is of interest in relation to repair and maintenance procedures. A continuous layer formed by deposition products is present on specimens exposed in the cold section of the loop. At isolated places the deposits are separated from the matrix by an oxygen containing phase. No interaction of substitutional elements of the deposit with the substrate could be stated by metallographic techniques. The deposition layer has a porous structure and a very irregular thickness varying between 2.10^{-6} and 10^{-5}m after 7275 h exposure at 355°C during the low-velocity corrosion experiments.

The morphology of the deposition layer found after the high-velocity experiments is identical.

3.3.3. Chemical changes

Concentration-penetration profiles and the composition of individual phases present in the deposition layer have been determined by microprobe analyses and by the RSV method [5]. The deposits are rich in iron ; the composition of the deposition layer at the interface with the matrix is as follows : Fe = 97.60 wt.% ; Cr = 0.65 wt.% ; Ni = 1.70 wt.% ; Mn = 0.03 wt.% and Si = 0.009 wt.%. The outer side of the deposit in equilibrium with lithium corresponds roughly with pure iron. The RSV method revealed the presence of calcium especially at the substrate-deposit interface. Carbon was found to be present throughout the whole deposition layer. The mean concentration of carbon in the deposition layer is 0.5 wt.%.

3.3.4. Structural and scanning electron microscope analyses

The surface of the deposition samples has been examined by X-ray analyses and by a scanning electron microscope equipped with an EDAX system.

The surface of the specimens exposed in the cold test section reveals the presence of crystalline iron-rich deposits with α-Fe structure. At certain places deposits rich in Cr and alloyed with Ca, Fe and Si are found to be present.

4. Discussion and conclusions

From the weight changes it is obvious that considerable mass transfer occurs even at temperatures as low as 400°C ; the mass transfer being closely related to the purity of the lithium. The accelerated corrosion stated in impure lithium (high cold trap temperature, ineffective low-temperature gettering) is due to the increased solubility of alloy constituents in lithium with higher nitrogen contents [2]. Carbon has no influence on the solubility of substitutional elements in dynamic lithium but promotes accelerated attack of stainless steels due to the enhanced attack of nickel-rich areas resulting from the formation of carbides at the grain boundaries.

Titanium not only reduces the nitrogen content of lithium but to a lesser extent oxygen, hydrogen and carbon. The formation of an impervious oxinitride layer is partly responsible for the low gettering capacity of FeTi alloys.

Ineffective gettering of lithium results not only in a considerable decrease in wall thickness of structural materials tested in dynamic lithium at low temperature but also in a com-

plete deterioration of the metallographic structure in the subsurface layer of the austenitic stainless steels in contact with lithium.

The corrosion rate is found to be a function of the lithium velocity, temperature and the effectiveness of the gettering mechanism.

The measured corrosion rates are rather large compared to previously published values. However, most of earlier experiments have been carried out in small-scale thermal convection loops [1][6], in which higher lithium purity levels could be obtained.

The comparison with previously published results is difficult since flow rates, time of tests, thermal treatments and stainless steel composition interfere with the resulting corrosion rates. Dynamic lithium provokes furthermore the formation of a low density ferritic subsurface layer with low mechanical strength. This layer extends at 400°C up to 10^{-5}m depth which is practically independent of exposure time, lithium velocity and the exact composition of the austenitic grade. The thickness reaches 15.10^{-5}m after 1200h exposure at 600°C.

The formation of this subsurface layer is due to the selective leaching of steel alloying elements such as chromium, nickel, molybdenum, manganese in lithium and the pick-up of calcium, lithium, carbon and nitrogen from the lithium.

The increase of the corrosion rate in impure lithium is caused by the increased solubility of the alloy constituents in lithium. The presence of lithium in the reaction layer is promoted by the high carbon and nitrogen content of the lithium, resulting in an enhanced intergranular attack. The nitrogen and carbon pick-up is in accordance with thermodynamic data of the Li-N, Li-C, Fe-Cr-Ni-C and Fe-Cr-Ni-N systems [4][7][8].

The surface morphology reveals the presence of holes (pitting) developing from the inner of the material towards the surface. The most likely reason for the occurrence of this lithium corrosion effect is the interaction of interstitial compounds present in the ferritic layer with penetrating lithium. The reaction products possess a lower density and give rise to a bulging effect.

The specimens exposed in the cold sections of the loop gain weight, due to the deposition of particles on their surface. These particles have a crystalline character and consist practically of pure iron slightly alloyed with carbon.

The absence of other steel constituents in the deposits in the cold section of the loop is associated with the complex thermodynamic relationships between lithium, dissolved corrosion products, the substrate and temperature throughout the loop. The increased solubility of alloy constituents of the steel in liquid lithium compared to sodium results in a much higher corrosiveness of dynamic lithium.

Acknowledgements

The authors wish to acknowledge Euratom for its financial support.

References

[1] DEVAN J.H., SELLE J.E., MORRIS A.E., "Review of lithium iron-base alloy corrosion studies", ORNL-TM-4927, (1976).

[2] MARONI V.A., CAIRNS E.J. and CAFASSO E.A. "A Review of the Chemical, Physical and Thermal Properties of lithium that are related to its use in fusion reactors", ANL-8001, (1973).

[3] LIEVENS F., PARMENTIER C., SOENEN M. "Sodium Characterization during the starting period of a sodium loop", Proceedings International Conference on liquid metal Technology in

Energy Production., Champion, 3-6 May 1976, CONF-760503, 105-111.

[4] SMITH D.L. and NATESAN K., "Influence of nonmetallic impurity elements on the Compatibility of liquid lithium with potential CTR containment materials", Nuclear Technology 22,392-404 (1974)

[5] SCHNEIDER H., "Investigations of changes in the surface layer composition of materials exposed to sodium by glow discharge optical and Auger Electron Spectroscopy". Proceedings International Conference on liquid Metal Technology in Energy Production Champion, 3-6 May 1976, CONF-760503, 716-722.

[6] SELLE J.E., "Corrosion of iron-base alloys by lithium", International Conference on Liquid Metal Technology in Energy Production, Champion 3-6 May 1976, CONF-760503 453-461.

[7] NATESAN K. and KASSNER T.F., "Thermodynamics of carbon in nickel, iron-nickel and iron-chromium-nickel alloys". Met.Transactions 4, 2557-2566 (1973).

[8] BLAZEJAK D., HERSLEB G., WESTERFELD K.J., Löslichkeit von Stickstoff in Fe-Cr-Ni Legierungen, Werkstoffe u. Korrosion 27, 398-406 (1976)

Table I

Chemical composition of exposed alloys

Alloy designation	Composition (wt.%)						
	Cr	Ni	Mn	Mo	Si	C	N
AISI 304	18.12	8.34	1.44	0.08	0.416	0.048	0.0465
AISI 304 L	17.80	9.10	1.10	0.155		0.0193	0.0195
AISI 316	17.80	10.8	1.63	2.13	0.56	0.03	0.0315
AISI 316 L	15.70	12.55	0.69	2.90		0.0202	0.161
Carbon steel		0.015	0.25		0.05	0.037	0.003

Table II

Analysis of lithium and Ti sponge for the different test periods

Period	Lithium				Ti sponge	
	Carbon (ppm)			Nitrogen (ppm)	Nitrogen (ppm)	(as received) (29 ppm)
	as carbide	as carbonyl	as carbonate			
4	377	37	1.4	1860	260 ppm (50 g exposed at 400°C)	
7 (at end)				outer side 69000 (200g exposed at 600°C)	inner side 57000	

Table III

Evolution of cold trap temperature as a function of exposure time in the different test periods

Test period	Total duration of test period (h)	Time with cold trap temperature above 190°C (h)	lithium velocity in hot section $m.s^{-1}$	lithium velocity in cold section $m.s^{-1}$
4	745	624	0.128-0.141	0.128-0.140
5	1827	181	0.142-0.156	0.121-0.133
6	2161	240	0.264-0.271	0.121-0.133
7	2542	100	0.264-0.271	0.121-0.133
8	811	100	1.60	0.03
9	1586	100	2.375	0.09
10	3262	100	2.23	0.08

Table IV.A.

Corrosion rate of structural materials in dynamic lithium during the different periods

Material	Pre-corrosion heat treatment	Corrosion rate ($10^{-6}m.a^{-1}$) for different test periods (velocity expressed in $m.s^{-1}$)		
		4(0.128-0.146)	5(0.142-0.156)	6 + 7 (0.264-0.271)
AISI 304		20.80	10.80	
AISI 316		23.84	9.98	14.61
AISI 316	15min/1050°C		13.23	
AISI 316L				21.66

Table IV.B.

Corrosion rate of structural materials in dynamic lithium during different test periods

Material	Heat treatment	Corrosion rate ($10^{-6}m.a^{-1}$) during different test periods (velocity expressed $m.s^{-1}$)				
		8(1.68$m.s^{-1}$)	9(2.375$m.s^{-1}$)		10(2.23$m.s^{-1}$)	
			pre-corroded		pre-corroded	
AISI 316		77.89	70.36	66.96	28.4	27.8
AISI 316	15min/1050°C	78.58	70.52	63.38	27.4	29.2
AISI 316	15min/1050°C and 24h at 700°C	76.16	70.65	65.95	25.6	30.1
AISI 316L	precorroded in lithium during 6673h	88.22	74.67		34	
AISI 316L	15min/1050°C and 24h at 700°C	77.89	71.02	68.16	28.4	29.8
AISI 304	15min/1050°C and 24h at 700°C	69.06	70.92	67.12	30.4	26.1
AISI 304L	15min/1050°C and 24h at 700°C	67.51	68.22	60.81	26.9	26.3
Carbon steel		106.14	108.22		40.1	

Table V.A.

Deposition rate on different substrates during low velocity experiments

Material	Heat treatment	Deposition rate ($10^{-6}m.a^{-1}$) during different test periods	
		test period 4	test period 5+6+7
AISI 304		+ 1.73	+ 3.36
AISI 316	15min/1050°C	0	+ 2.23

Table V.B.
Deposition rate on different substrates in dynamic lithium during different test periods

Material	Pre-corrosion treatment	Deposition rate (10^{-6}m.a^{-1}) during different test periods		
		8	9	10
AISI 304		+ 5.47	+ 6.35	+ 1.18
Carbon steel		+ 3.04	+ 6.44	+ 1.40
AISI 316	10min/1050°C and 24h at 700°C	+ 8.69	+ 3.20	+ 0.64

Table VI
Composition of bulk material and corrosion layers of AISI 304 and AISI 316 exposed for 2572h to 400°C lithium (wt.%)

Elements	Bulk material AISI 304	Ferritic zone in equilibrium with	
		bulk material	lithium
Fe	72.55	91.06	92.00
Cr	17.16	7.35	4.71
Ni	8.71	1.10	1.10
Mn	0.83	0.14	0.07
Si	0.44	0.24	0.24
Mo	0.31	0.11	0.11

Elements	Matrix AISI 316	Porous layer	Fe-rich layer in equilibrium with	
			lithium	Places of enhanced corrosion
Fe	67.35	80.96	94.05	99.37
Cr	17.06	5.47	1.90	0.10
Ni	11.05	0.89	0.81	0.06
Mn	1.72	0.06	0.03	0.46
Si	0.75	0.99	0.04	0.00
Mo	2.07	1.19	0.00	0.00
balance (porosities)		(10.44)	(3.6)	

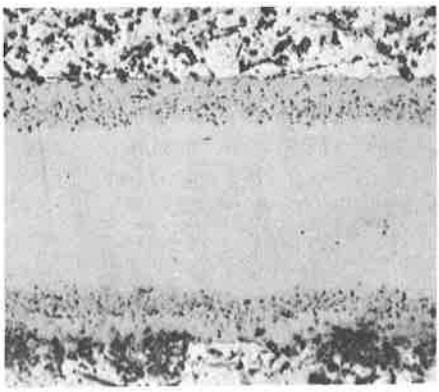

AISI 304-2572h(0.14)

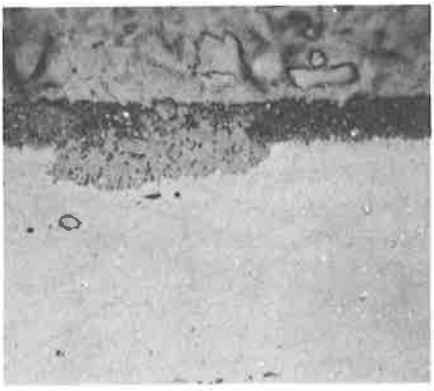

AISI 316L-4101h(0.27)

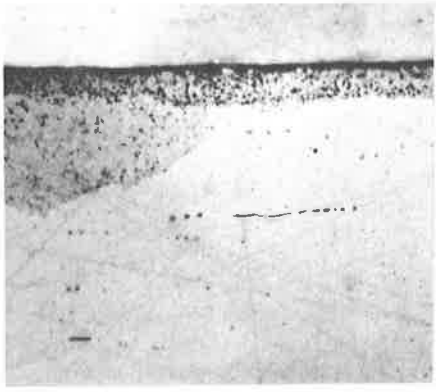

AISI 316-6673h(0.26)

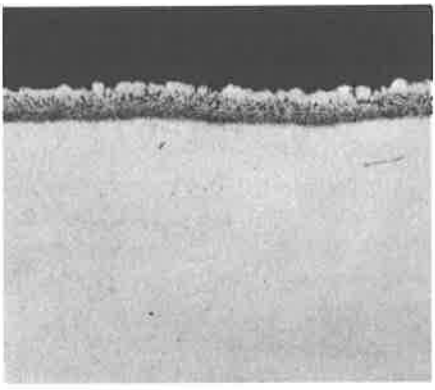

AISI 316-811h(1.60)

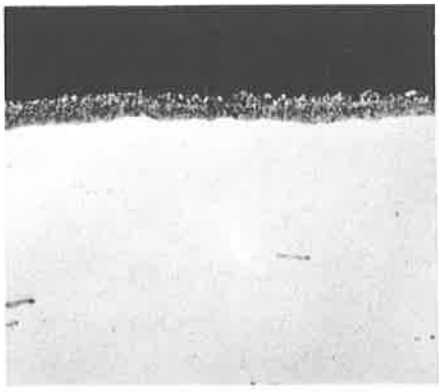

AISI 316-1586h(2.375)

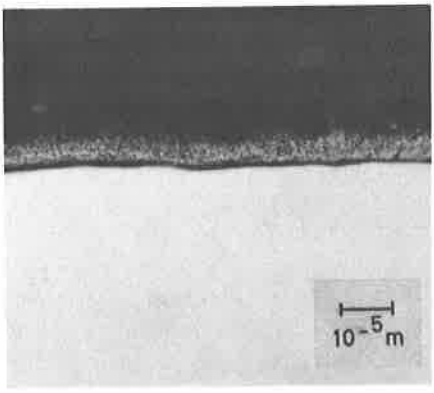

AISI 316-2397h(1.60-2.375)

Fig. 1. : Metallographies of steel-lithium interface of structural materials exposed to 400°C lithium as a function of exposure conditions (time and velocity ($m.s^{-1}$)